Supplementary information for

High flux high-silica SSZ-13 membrane for CO_2 separation

Nikolay Kosinov[a], Clement Auffret[a], Canan Gücüyener[b], Bartłomiej M. Szyja[c], Jorge Gascon[b], Freek Kapteijn[b] and Emiel J.M. Hensen[a]*

[a] Schuit Institute of Catalysis, Laboratory of Inorganic Materials Chemistry, Eindhoven University of Technology, PO Box 513, 5600 MB Eindhoven, The Netherlands. E-mail: e.j.m.hensen@tue.nl, tel: +31-40-2475178
[b] Catalysis Engineering, ChemE, Delft University of Technology, Julianalaan 136, 2628 BL Delft, The Netherlands.
[c] Institute for Solid State Theory, University of Münster, Wilhelm-Klemm Str. 10, 48149 Münster, Germany.

* Corresponding author

Table of contents

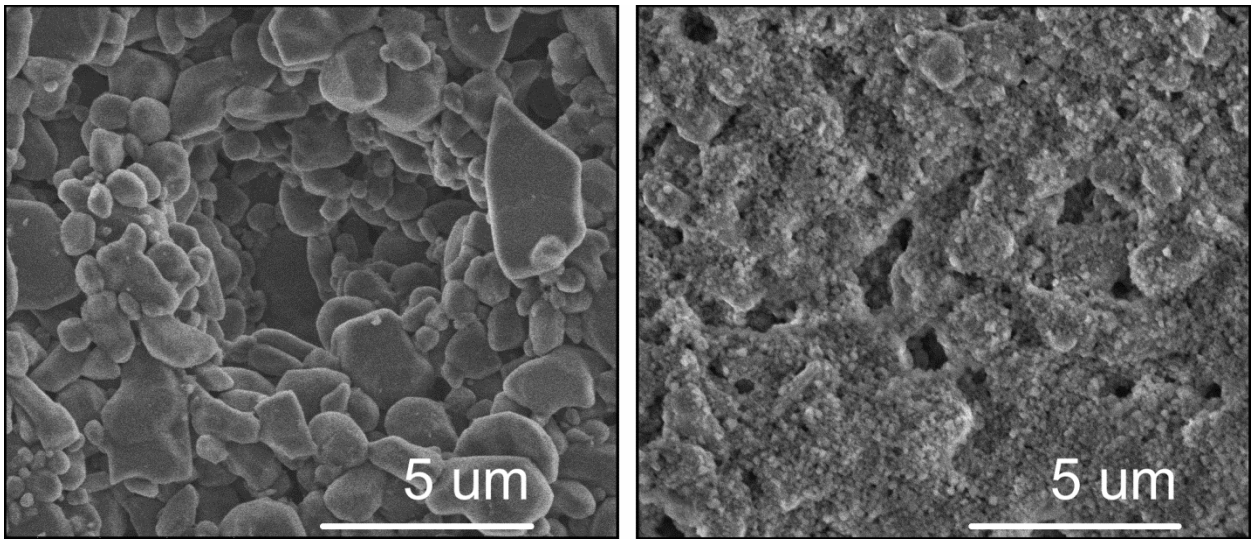

Fig. S1 SEM images of the macroporous α-alumina support surface (*left*) and layer of SSZ-13 seed crystals after two dip-coating steps (*right*).

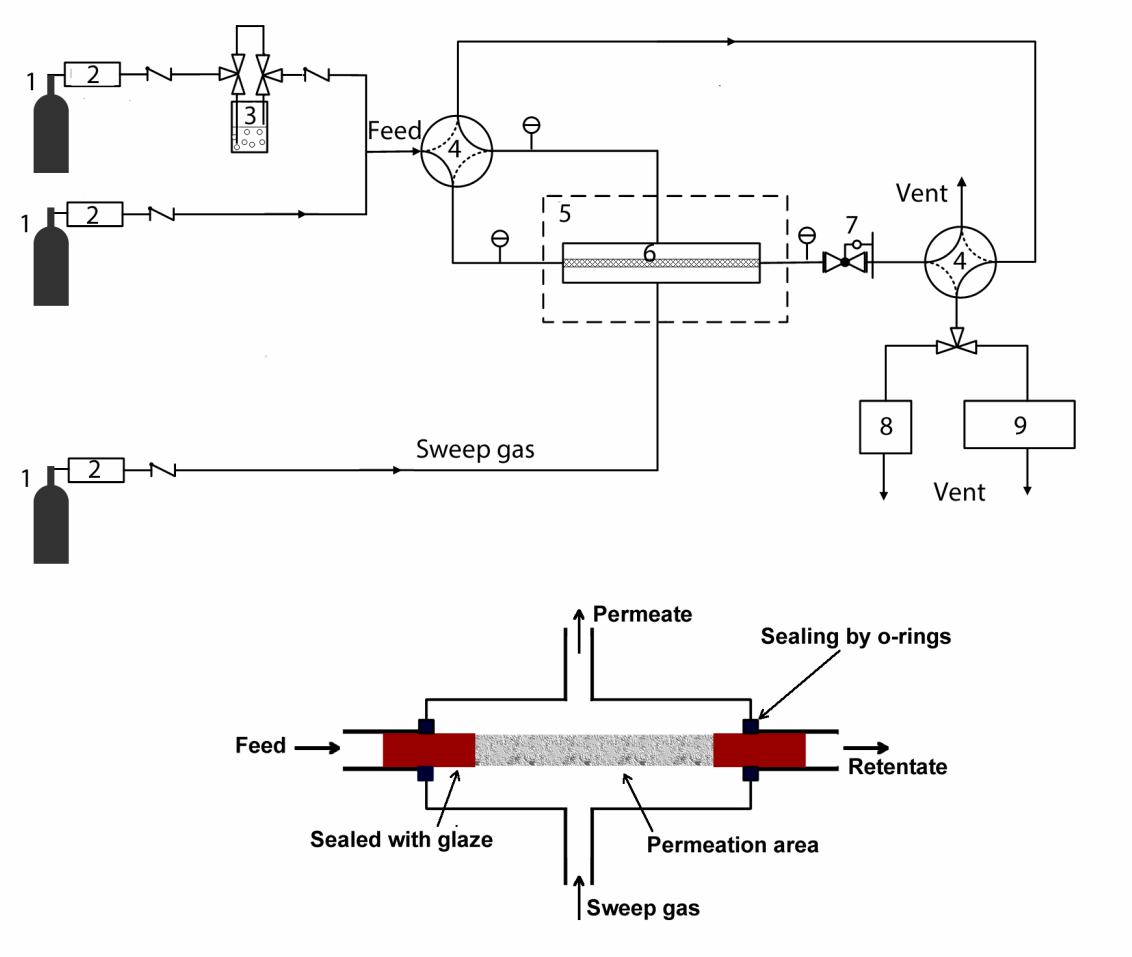

Fig. S2 Scheme of separation setup and membrane module.

1. Gas bottles
2. Mass-flow controllers
3. Stainless steel saturator
4. 4-way valves
5. Oven
6. Membrane module
7. Back-pressure regulator
8. Flow meter (digital or bubble)
9. Online GC

Calculation of permeance

Due to use of hollow fiber membranes the composition of the feed flow may change along the membrane length. To account for that we used log-mean pressure difference calculated as follows:

$$(\Delta p_i)_{ln} = \frac{\left(p_i^{feed} - p_i^{perm}\right) - \left(p_i^{ret} - p_i^{perm}\right)}{\ln\left(\frac{p_i^{feed} - p_i^{perm}}{p_i^{ret} - p_i^{perm}}\right)}$$

Retentate, permeate and feed flows and compositions were measured for every experiment and the values were applied for the above calculation.

The back-permeation of sweep gas was neglected in this work. It may, however, significantly influence the membrane performance, especially at lower pressures [J.M. van der Graaf, et al. *J. Membr. Sci*., 1998, **144**, 87-104 and J. van der Bergh et al., *J. Membr. Sci.,* 2008, **16,** 35]. Hence, we are currently investigating this effect, to be published in a follow-up publication [C. Gücüyener et al., *Modeling permeation of binary gas mixtures across an SSZ-13 zeolite membrane,* in preparation]

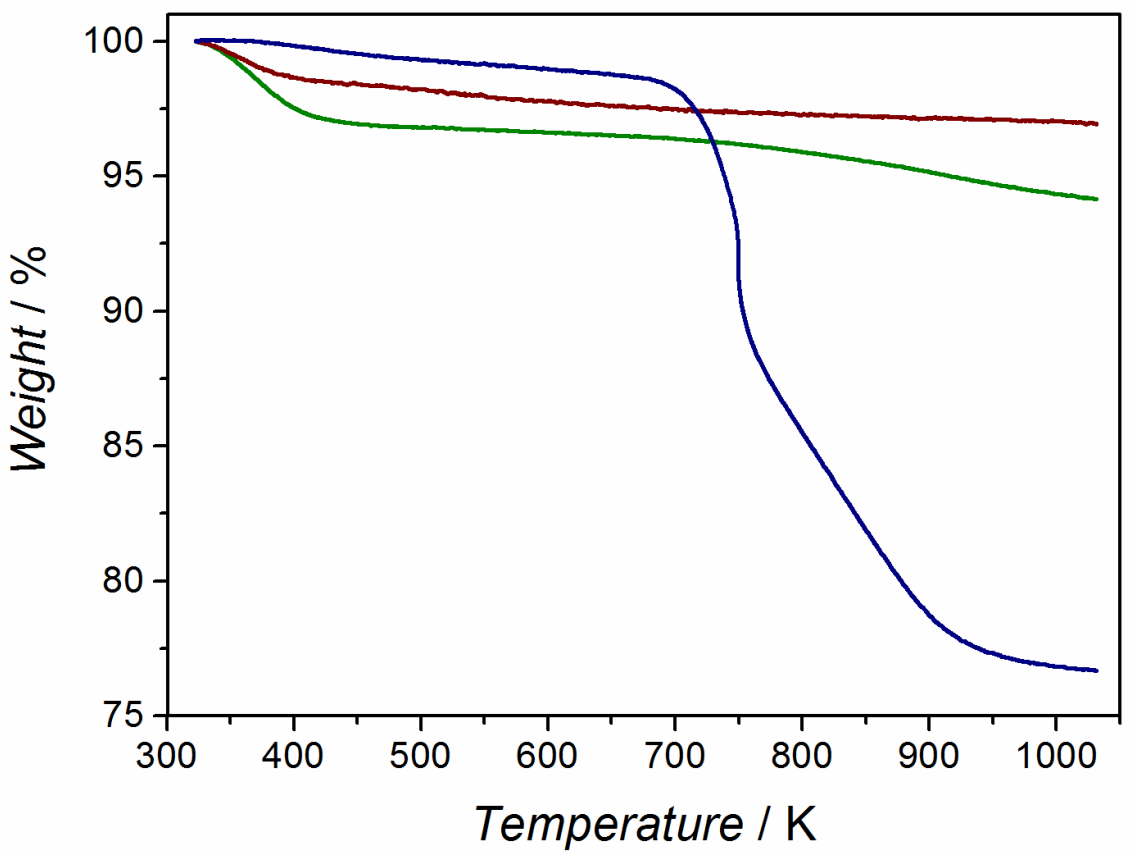

Fig. S3 TGA curves of SSZ-13 powder (Si/Al=100) calcined in air at 700°C for 5 h (red); calcined in oxygen at 450°C for 80 h (green) and as-synthesized (blue). Heating rate 5 K/min, air flow 40 ml/min.

Table S1 Weight loss of different SSZ-13 samples

Sample	Weight loss (400°C-750°C), %
Calcined at 700°C	0.6
Calcined at 450°C	2.3
As-synthesized	22.0

Detemplation extent: 92.3%

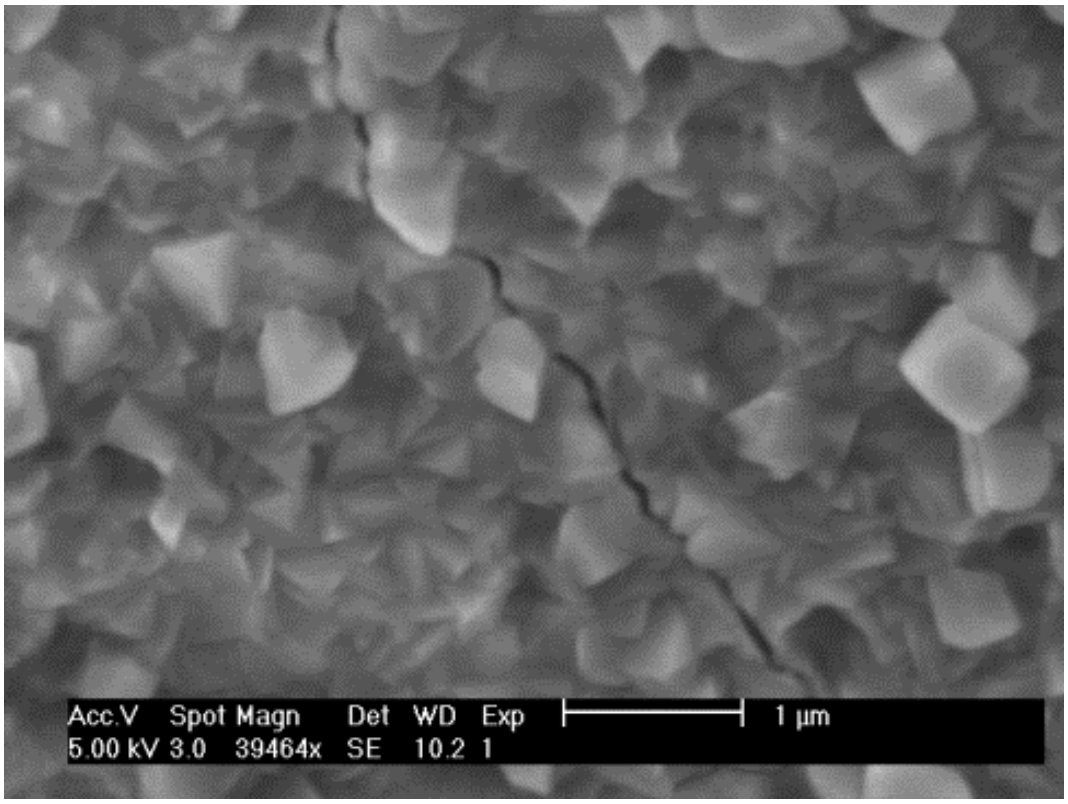

Fig. S4 SEM image of a crack formed on the membrane surface after calcination at 550°C in artificial air flow.

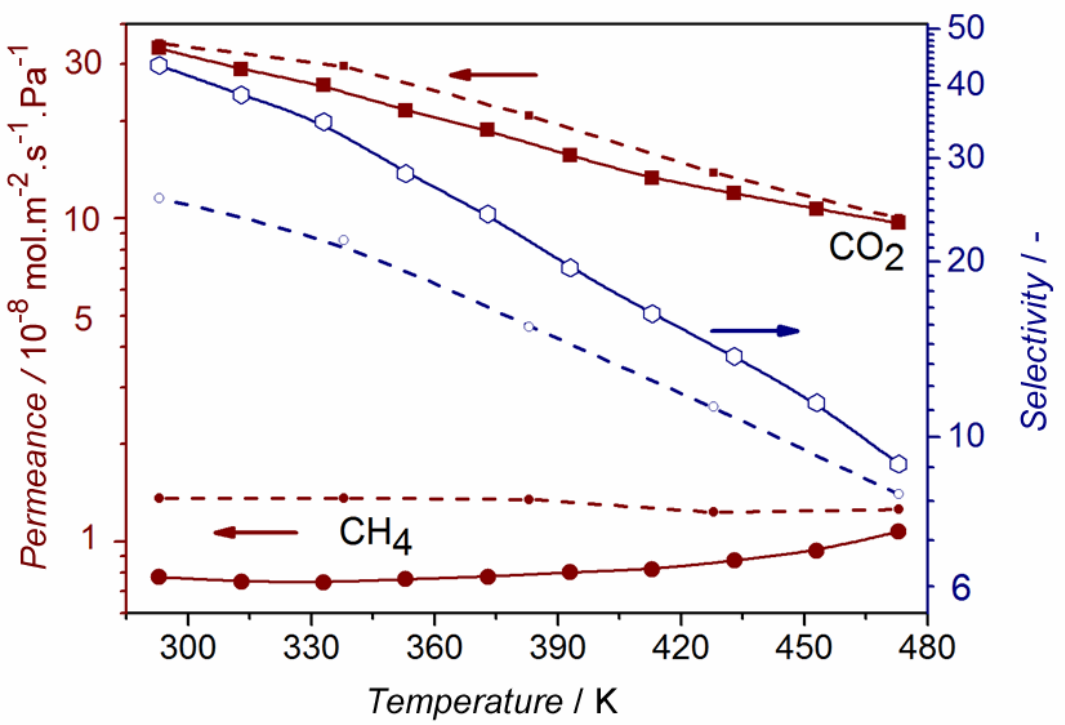

Fig. S5 CO_2/CH_4 equimolar mixture separation in a pressure gradient mode with no sweep gas (dashed lines - single component permeance and ideal selectivity, solid lines - mixture separation results; conditions: 0.6 MPa feed pressure, atmospheric pressure at permeate side, total feed flow rate 200 ml/min.).

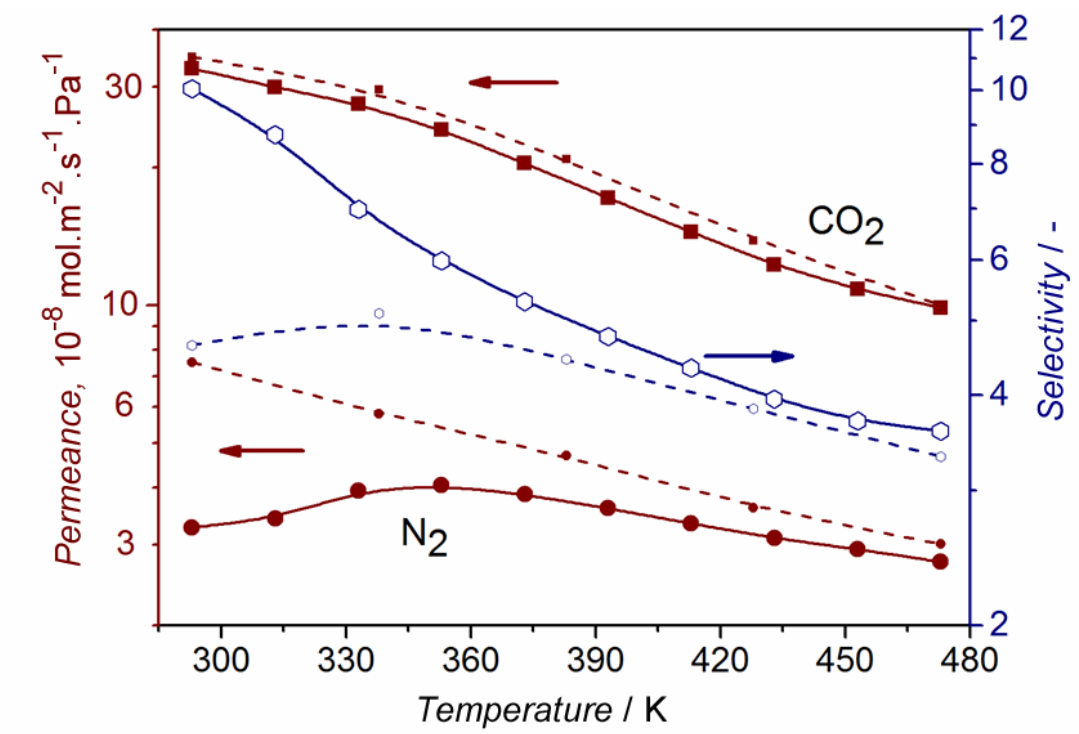

Fig. S6 CO_2/N_2 equimolar mixture separation in a pressure gradient mode without sweep gas (dashed lines - single component permeance and ideal selectivity, solid lines - mixture separation results; conditions: 0.6 MPa feed pressure, atmospheric pressure on permeate side, total flow rate 200 ml/min)

In the pressure mode at 6 bar total feed pressure without using a sweep gas results were very similar to those obtained in the sweep-gas mode for both mixtures separations. The flux at lower pressures and especially in the presence of water was not high enough to provide reliable GC analysis. Thus, sweep-gas mode was chosen as the standard in this work.

The temperature dependencies presented in Figures S5 and S6 reveal the following trends. For the single component permeation the CO_2 permeance decreases with temperature, as a result of the decreasing concentration in the membrane. For CH_4 the permeance is nearly constant, which may be caused by the combined influence of activated diffusion and permeation through defects. The nitrogen permeance passes through a maximum which can be the result of a slightly activated diffusion process and a decreasing concentration in the membrane, similarly as for MFI and DDR membranes. [F. Kapteijn et al., *AIChE J.,* 2000, **46,** 1096 and J. van der Bergh et al., *J. Membr. Sci.,* 2008, **16,** 35]

For both mixtures the selectivity monotonically decreases and evolves to that of the ideal selectivity at higher temperatures. For CO_2/CH_4 the mixture selectivity is lower, due to an increased permeance of methane, suggesting an interaction with the faster permeating carbon dioxide. For the CO_2/N_2 selectivity this 'entrainment' of N_2 seems even stronger at lower temperatures, resulting in an appreciable lower selectivity at low temperatures, passing through a weak maximum as a function of temperature.

The preparation of SSZ-13 membranes on the supports with higher permeation area can ensure permeation flows high enough to perform the separation in the pressure gradient mode at lower pressures [Canan Gücüyener et al., *Modeling permeation of binary gas mixtures across an SSZ-13 zeolite membrane,* in preparation].

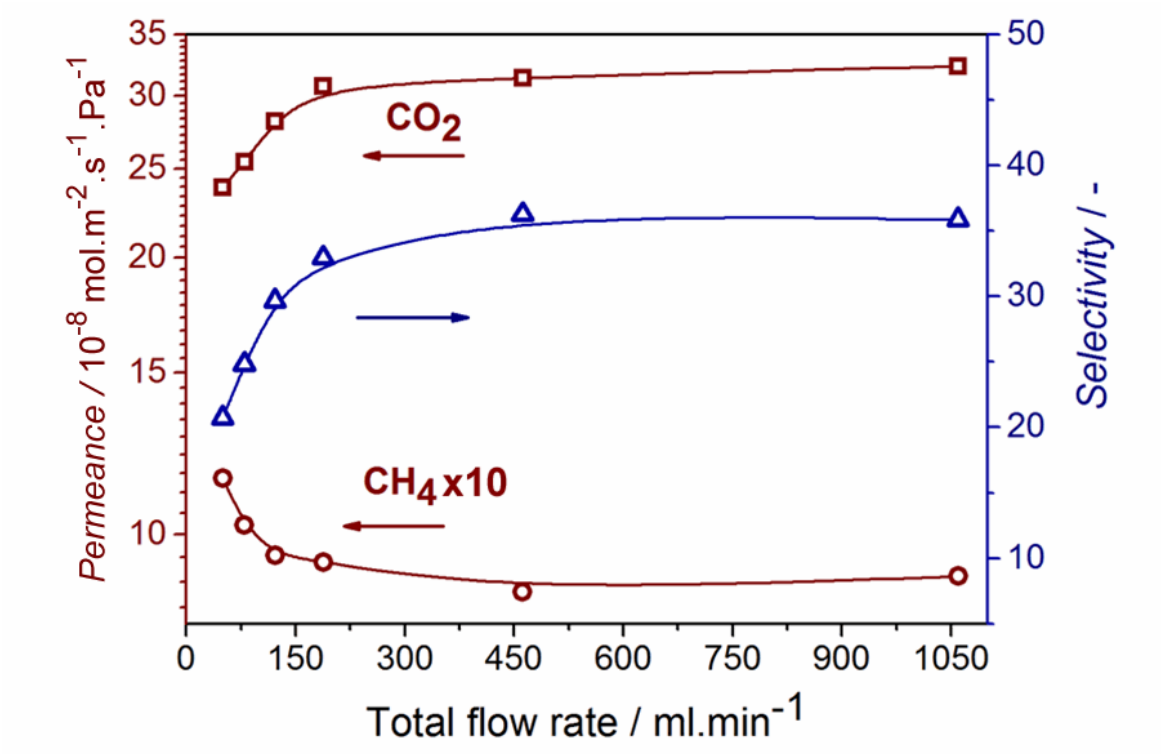

Fig. S7 Influence of total flow rate on SSZ-13 membrane separation of an equimolar CO_2/CH_4 mixture (conditions: 293 K, 0.6 MPa feed pressure, atmospheric pressure on permeate side, 200 ml/min of sweep gas).

To avoid influence of a concentration-polarization effect the flow rate of 200 ml/min was chosen as the standard for the permeation and separation tests.

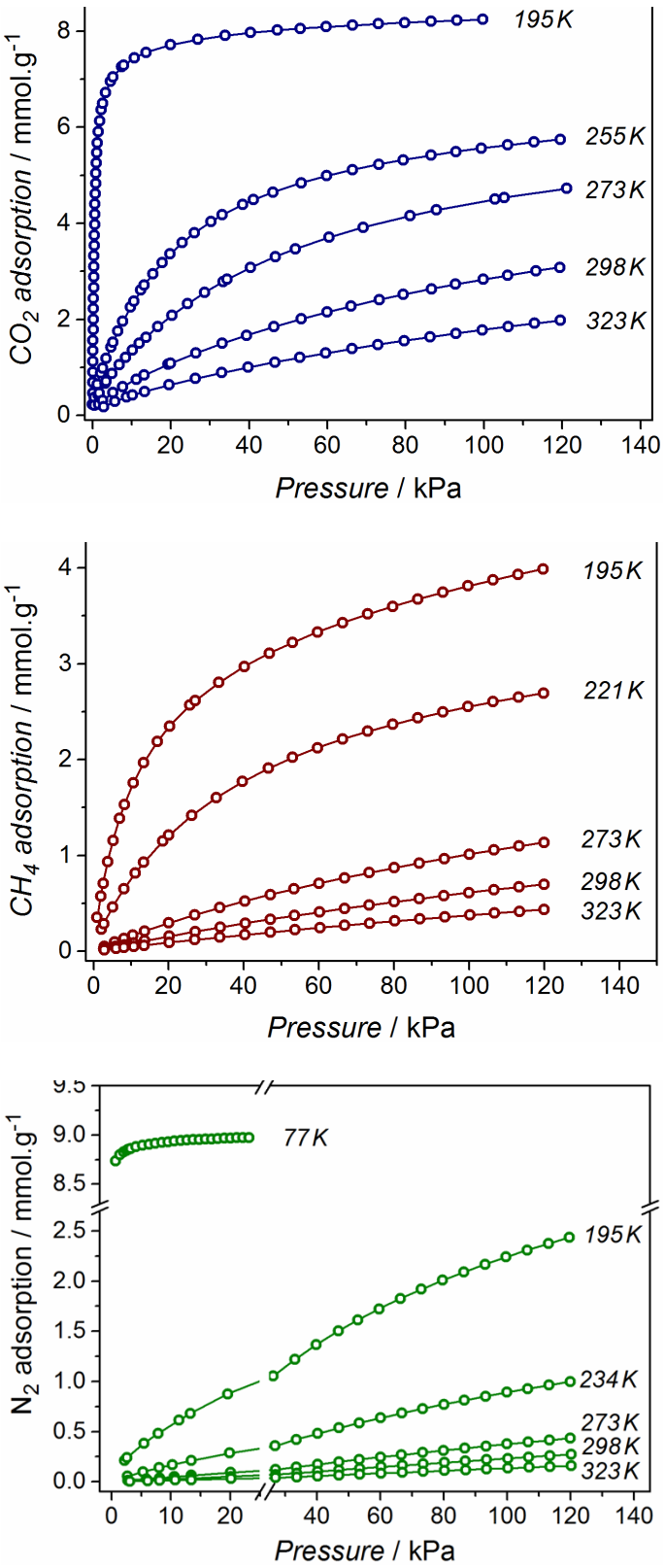

Fig. S8 CO_2, CH_4 and N_2 adsorption isotherms of SSZ-13 powder (Si/Al=80).

Estimated dual site Langmuir adsorption parameters of CO_2, CH_4 and N_2 for SSZ-13 (Si/Al =80); including their 95% confidence intervals.

Adsorbate	***# of sites***	$q_i^{sat,A}$ **mol kg^{-1}**	$-\Delta H_i^A$ **kJ mol^{-1}**	$K_{0,i}^A$ **10^{-7} kPa^{-1}**	$q_i^{sat,B}$ **mol kg^{-1}**	$-\Delta H_i^B$ **kJ mol^{-1}**	$K_{0,i}^B$ **10^{-7} kPa^{-1}**
CO_2	2	3.78±0.75	32.0±1.70	0.03±0.03	4.32±0.75	24.8±0.72	6.73±2.97
N_2	2	1.46±0.26	19.3±1.49	2.99±2.07	7.50±0.26	10.6±0.19	23.4±5.52
CH_4	2	3.05±0.16	19.7±0.59	0.43±0.22	2.66±0.14	17.9±0.11	20.5±1.02

Following cooling baths were employed to achieve the desired temperatures for adsorption:

Adsorption at 195 K – Isopropanol/Ice

Adsorption at 221 K – Ethylene glycol / Ethanol / Solid CO_2

Adsorption at 234 K – Ethylene glycol / Ethanol / Solid CO_2

Adsorption at 255 K – Kryo 20

Adsorption at 273 K – Ice

Adsorption at 298 K – Water

Adsorption at 323 K – Heating

In adition, Ar phisysorption tests at 87 K were performed on an SSZ-13 sample with an Si/Al ratio of 86 to evaluate its textural properties. BET surface of the sample is 632 $m^2.g^{-1}$ and microporous volume calculated by *t*-plot model is 0.25 $cm^3.g^{-1}$.

Computational details

In addition to description given in the main text, the interactions between the various molecules are described in a pair-wise fashion using the following parameters:

Center i	Center j	R0 [Å]	D0 [kcal/mol]
CH4	O_z	3.895	0.2285
CH4	CH4	4.176	0.3150
CH4	C_CO2	3.637	0.1327
CH4	O_CO2	3.794	0.2245
CH4	N	3.951	0.1509
C_CO2	O_z	3.122	0.0998
C_CO2	C_CO2	3.098	0.0559
C_CO2	O_CO2	3.244	0.0946
C_CO2	N	3.412	0.0636
O_CO2	O_z	3.277	0.1688
O_CO2	O_CO2	3.404	0.1600
O_CO2	N	3.569	0.1076
N	O_z	3.437	0.1158
N	N	3.727	0.0723

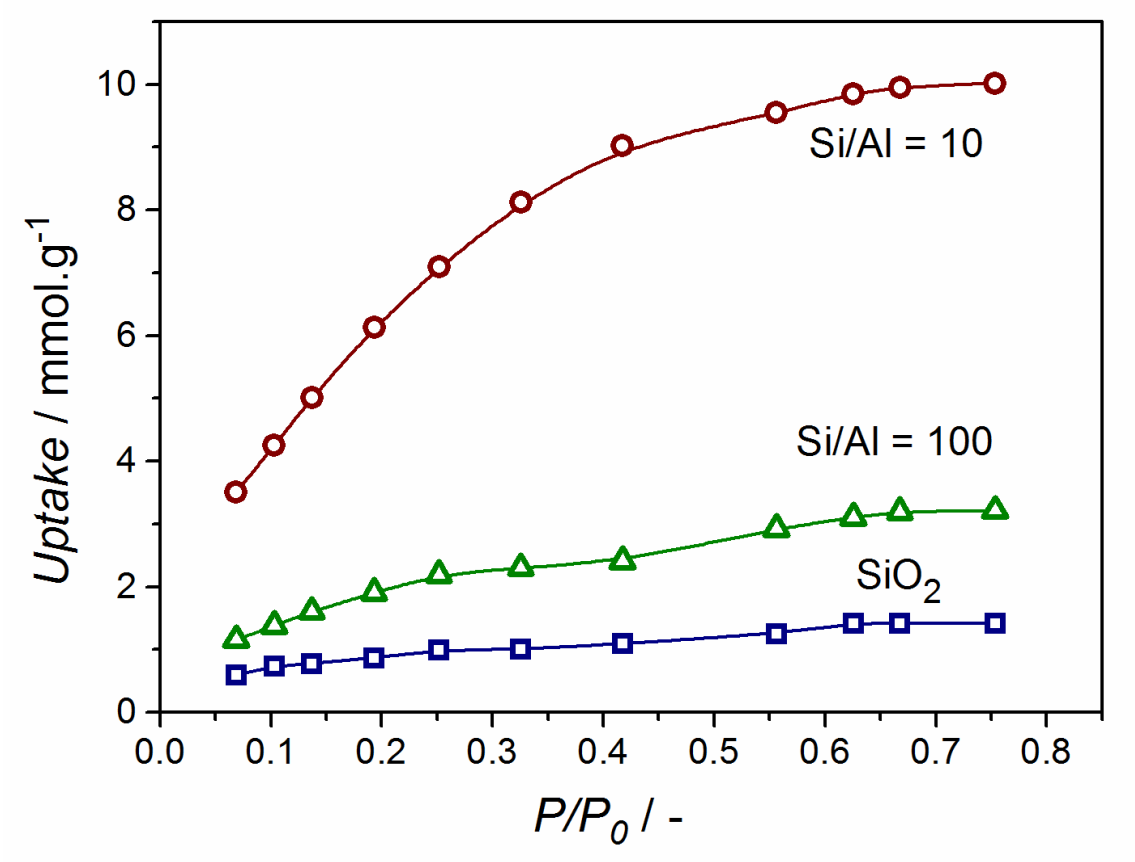

Fig. S9 Water adsorption isotherms of SSZ-13 samples of different synthesis Si/Al ratios at 298 K, measured by gravimetry.

A detailed description of the adsorption procedure can be found in [N. Kosinov et al. *Microporous Mesoporous Mater.* (2014) *in press,* doi: http://dx.doi.org/10.1016/j.micromeso.2014.03.034]

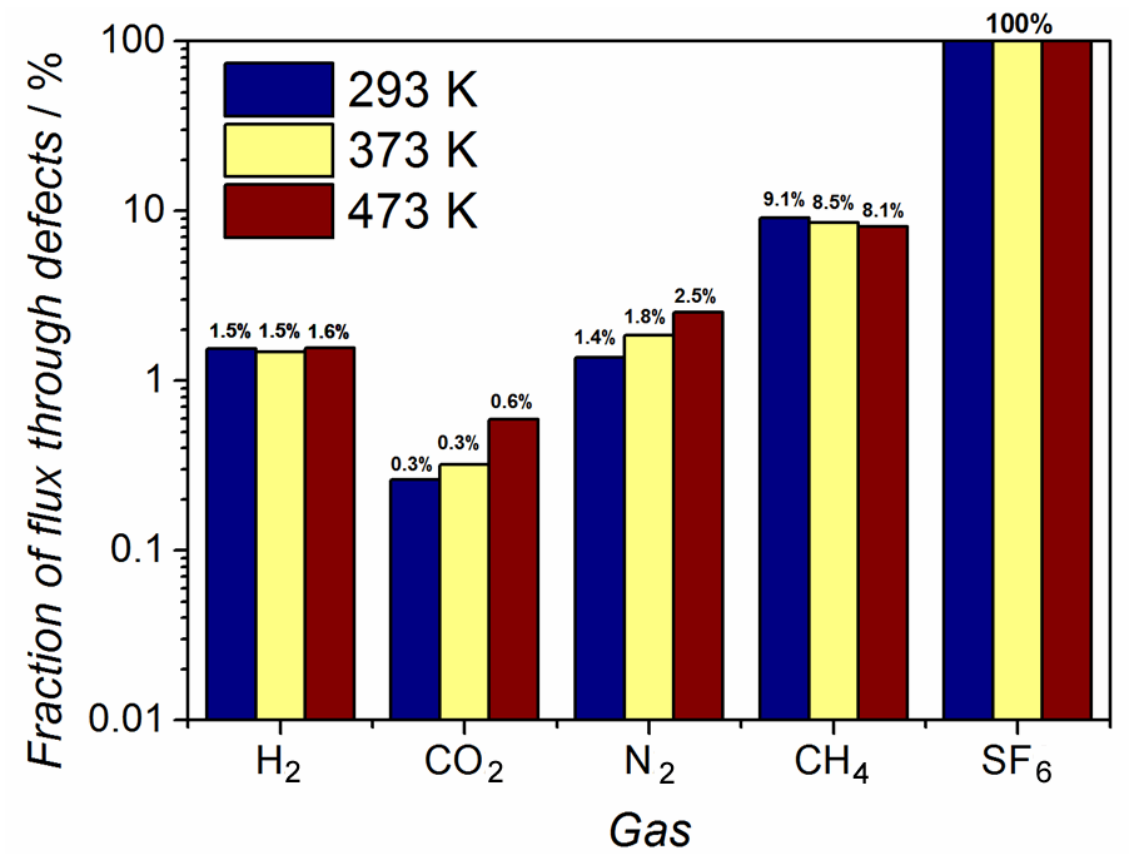

Fig. S10 Contributions of defect flow for different gases derived from single-gas permeation data.

SF_6 is assumed to permeate exclusively through defects by Knudsen diffusion, and therefore the contribution of the defect permeance for other gases is calculated as:

$$\Pi^{i} = \Pi^{SF_6} \cdot \sqrt{\frac{Mr\,(SF_6)}{Mr(i)}}$$

where Π^{i} – permeance of gas *i*, $Mr(i)$ – molecular mass of gas *i*.